2004-06

Experimental and computational investigation of cross-flow fan propulsion for lightweight VTOL aircraft

Hobson, Garth V.; Cheng, W.T.; Seaton, M. Scot; Gannon, Anthony; Platzer, Max F.

ASME

G.V. Hobson, W.T. Cheng, M. Scot Seaton, A. Gannon, M.F. Platzer, "Experimental and computational investigation of cross-flow fan propulsion for lightweight VTOL aircraft," Proceedings of ASME Turbo Expo 2004, Power for Land, Sea and Air, June 14-17 2044, Vienna, Austria, GT2004-53468, 11 p.

http://hdl.handle.net/10945/55391

Proceedings of ASME Turbo Expo 2004
Power for Land, Sea, and Air
June 14-17, 2004, Vienna, Austria

GT2004-53468

EXPERIMENTAL AND COMPUTATIONAL INVESTIGATION OF CROSS-FLOW FAN PROPULSION FOR LIGHTWEIGHT VTOL AIRCRAFT

Garth V. Hobson, W. T. Cheng, M. Scot Seaton, Anthony Gannon
and
Max F. Platzer
Turbopropulsion Laboratory
Naval Postgraduate School
Monterey, CA 93943

ABSTRACT

Cross-flow fan propulsion has not been seriously considered for aircraft use since an Vought Systems Division (VSD) study for the U.S. Navy in 1975. A recent conceptual design study of light-weight, single seat VTOL aircraft suggest that rotary-engine powered cross-flow fans may constitute a promising alternative to the conventional lift-fan vertical thrust augmentation systems for VTOL aircraft. The cross-flow fan performance data obtained by VSD supported the hypothesis that they could be improved to the point where their thrust augmentation could be used in a VTOL aircraft. In this paper we report results of a NASA Glenn supported experimental and computational cross-flow fan investigation which is currently in progress and we provide an assessment of the potential suitability of cross-flow fans for VTOL aircraft propulsion.

The tests are carried out in the Turbopropulsion Laboratory of the Naval Postgraduate School, using an existing Turbine Test Rig as a power source to drive the cross-flow fan. A 0.305 m (12-inch) diameter, 38.1 mm (1.5-inch) span cross-flow fan test article was constructed to duplicate as closely as possible the VSD fan so that baseline comparison performance data could be obtained. Performance measurements were taken over a speed range of 1,000 to 7,000 RPM and results comparable to those measured by Vought Systems Division were obtained. At 3,000 RPM a 2:1 thrust-to-power ratio was measured which dropped to one as the speed was increased to 6,000 RPM. Performance maps were experimentally determined for the baseline configuration as well as one with both cavities blanked off, for the speed range from 2,000 to 6,000 rpm. Using Flo++, a commercial PC-based computational fluid dynamics software package by Softflo, 2-D numerical simulations of the flow through the cross-flow fan were also obtained. Based on the performance measurements it was concluded that the optimum speed range for this rotor configuration was in the 3,000 to 5,000 rpm range. The lower speed producing the best thrust-to-power ratio and the upper speed range producing the highest efficiency over sizeable throttling range.

INTRODUCTION

The idea of using a paddle wheel to move a fluid is very old indeed and its realization resulted in the first mechanical means of ship propulsion, which is still in use today. The cross-flow fan may be regarded as a derivative of the paddle wheel, going back to a patent issued to the Frenchman Mortier in 1892. His fans were used in mine ventilation. Mortier was followed by a number of inventors who tried to improve his design. Most notable are the work initiated at the Aerodynamics Institute of the Federal Institute of Technology in Zurich under the direction of Prof. Ackeret [1], and the commercially viable cross-flow fans developed by Dr. Eck in Germany, who included a section

on cross-flow fans in his well-known textbook [2]. By the early 1960s, cross-flow fans became widely used in domestic appliances, such as fan heaters and miniature hand-held hairdryers. The principal advantage of cross-flow fans lies in the fact that there is no upper limit to their rotor length-to-diameter ratio, thus making it possible to specify a cross-flow fan of smaller diameter operating at higher speeds than comparable centrifugal fans, at a considerable space saving. It was this feature which stimulated Prof. Ackeret to consider cross-flow fans for use on airplane wings and it is this application which motivated the present investigation. Recently Peebles [3] demonstrated a Cross Flow Fan powered flying model.

CROSS-FLOW FAN BASICS

The cross-flow fan consists basically of a bladed cylindrical rotor closed at the ends and mounted in a housing defining the fan inlet and outlet, the housing extending the full length of the rotor. The blades are profiled and cambered forward in the direction of rotation so as to induce a flow across the rotor in a plane at right angles to the rotor axis. This type of fan generates a vortex located in the region where the blades pass from the fan outlet duct back to the fan inlet.

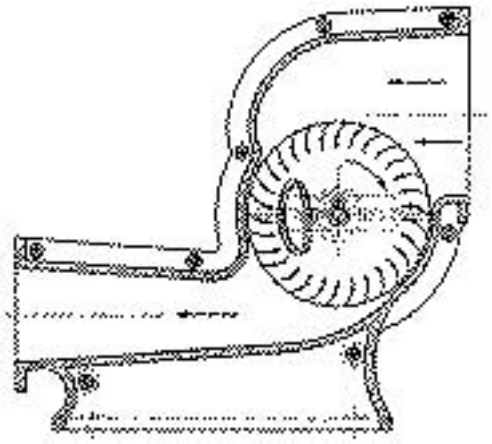

Fig. 1 Schematic of flow through the original Cross Flow Fan of Mortier [2].

CROSS-FLOW FAN (CFF) APPLICATIONS FOR VTOL AIRCRAFT

In his 1998 AIAA Dryden lecture Dennis Bushnell [4] pointed to the fact that society cannot easily continue to bear the costs imposed by almost sole reliance upon the automobile for short-to-intermediate passenger transport. He stressed the need for a personal air vehicle, and argued that the most promising vehicle is the vertical take-off and landing (VTOL) “converticar” that allows the user to land and take off from a relatively hard surface. He argued that the helicopter is the most likely configuration poised for development into a mass-produced personal air vehicle.

We agree with Bushnell that the “converticar” is the preferred vehicle. However, we believe that helicopters, while offering the best hovering efficiencies, have significant handling and safety disadvantages which make them less acceptable to the general public. We argue that a lift-fan powered fixed-wing aircraft is a more promising vehicle, trading reduced hovering efficiency for better cruise flight efficiency. Most importantly, ducted lift fans have the advantage of shielding users and bystanders from rotating blades and high noise levels. Lift-fan powered vehicles, whether manned or unmanned, are also likely to be of increasing interest for military and police applications due to their better handling characteristics and cruise efficiency.

This aspect has been recognized for many years. A company, Moller International of Davis, California, [5] is in the process of certifying a VTOL commuter airplane which uses four ducted fans with a thrust deflection vane system, enabling it to hover or to take off and land vertically. The fans are driven by rotary (Wankel) engines, which are small and have a good power-to-weight ratio. In cruise flight, approximately two thirds of the required lift is provided by the lift fans.

We agree with Moller International that the use of ducted fans is to be preferred over helicopter rotors and propellers. However, we argue that the conventional fixed-wing airplane configuration ought to be retained as much as possible to achieve good cruise flight efficiency and wider user acceptance. This raises the question whether there is still a configuration that has not yet been proposed and analyzed in the many past configuration studies.

Gossett [6] studied the feasibility of a single-seat VTOL airplane that could be used as a commuter vehicle. This aircraft was to have a range of 167 km (100 miles), a gross weight of 600 kg (1330 lbs) and a payload of 113 kg (250 lbs). He proposed to retain the deflected thrust ducted propellers powered by rotary engines used in Moller’s airplane as the main propulsion system. Two such ducted propellers provide 4.6 kN (1042 lbs) thrust. However; in contrast to

Moller's airplane which relies on four lift fans during the cruise flight portion, Gossett proposed a canard-wing configuration for the cruise flight, propelled by two ducted propellers. And to augment the thrust needed for VTOL with a cross-flow fan producing 3.1 kN (690 lbs) thrust. Key considerations therefore for the feasibility of the Gossett design are the thrust-to-volume, thrust-to-weight, and thrust-to-power characteristics achievable with cross-flow fans.

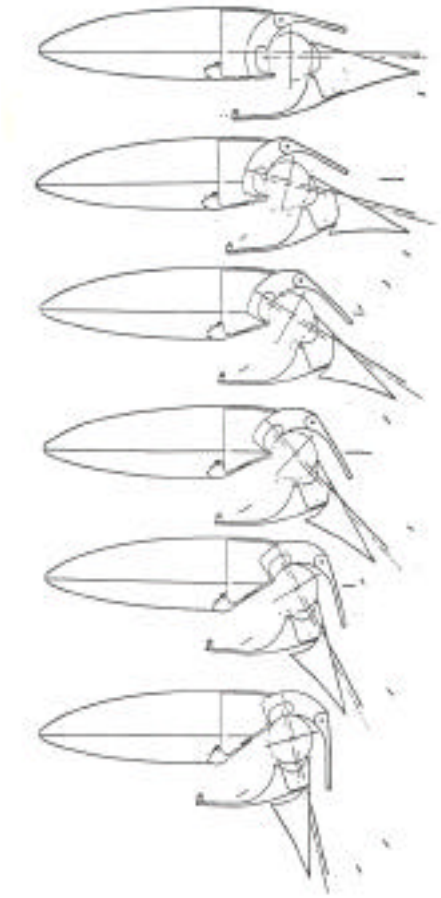

Fig. 2. Proposed in-wing thrust vectoring system, Vought [7].

An even more intriguing case for the use of cross-flow fans has been put forward by the Vought Systems Division of the LTV Aerospace Corporation in the 1970s [7]. At that time the US Navy was interested in the exploration of new concepts for the development of subsonic transport airplanes. Vought Systems considered Prof. Ackeret's original proposal to install cross-flow fans near the wing trailing edges for the purpose of attaining efficient lift augmentation during VTOL operation as shown in Figure 2. In this application the aforementioned flexibility of the CFF to install units having a small diameter together with a large span may offer significant advantages. It may make it possible to achieve an efficient thrust vectoring capability for vertical takeoff and landing because the fan discharge vector can be easily rotated about the fan axis. Also, for transition flight this arrangement has the advantage of achieving supercirculation because of the jet flap effect available from this type of installation. Finally, for cruise flight, the CFFs may offer advantages due the possibility of providing boundary layer suction and blowing.

The Vought Division, under contract to the Naval Air Systems Command, tested several fan configurations. Each fan had a diameter of 12 inches and was fabricated from aluminum with differing blade geometries and number of blades. Two different spans were tested, 38 mm (1.5 inch) and 0.305 m (12 inch) span. Also, various combinations of fan housing contours were tested. The instrumentation used for these tests was sufficient to determine the compression efficiency, pressure ratio and air mass flow rate, as a function of rotational speed. Furthermore, the inflow and exit flow distributions as well as the flow patterns within the rotor were measured.

PROJECT OBJECTIVES

The US Navy's diminishing interest after 1980 in the further development of subsonic VTOL airplanes led to the abandonment of further CFF studies. However, it stands to reason that the CFF is an underdeveloped fan, which should have significant development potential using modern computational analysis tools and measuring techniques. The optimum housing shape, blade design, blade number, rotational speeds, arrangement of the low- and high-pressure cavities remain to be determined. To achieve this objective, it appeared prudent to first establish baseline data against which improved designs could be evaluated. To this end, the Vought Systems CFF design was chosen as the baseline. In this paper we therefore report the experimental and computational results obtained for this baseline CFF.

CROSS-FLOW FAN DESIGN

The cross-flow fan rotor has a 0.305 m (12 inch) outer diameter and a 38 mm (1.5 inch) span. It was assembled from a machined disc with 30 identical rotor blade sections and a front retaining ring. Each blade was pinned in place using dowels and secured with Hysol epoxy E-120HP. Prior to assembly, the blades were

weighed and arranged in ascending order according to weight in order to minimize subsequent rotor balancing efforts. The rotor disc was designed to be recessed into the back plate, seating flush with the back wall of the assembly. A labyrinth seal on the tip of the rotor disc was used to minimize mass flow between the rotor and test assembly back plate cavity. Figure 3 depicts the fan in a partially assembled state. The external housing is shaped in such a way that it can accommodate two cavities and an exit duct, as shown in Figure 4. The exhaust duct height is 114 mm (4.5 in), with parallel walls. The front faceplate was also made of aluminum with Plexiglas inserts to enable viewing for flow visualization.

Fig. 3. Partially assembled 30 bladed rotor.

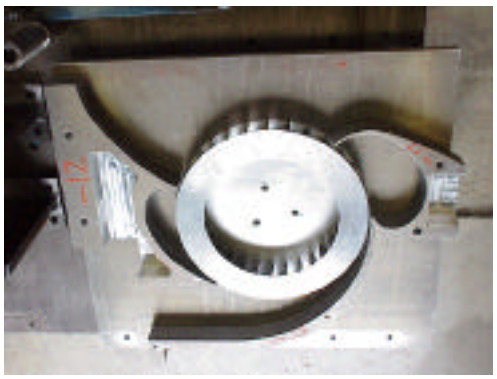

Fig. 4. Partially assembled Cross-Flow Fan.

DESCRIPTION OF CROSS-FLOW FAN TEST ASSEMBLY (CFTA)

The Turbine Test Rig (TTR) of the Naval Postgraduate School Turbopropulsion Laboratory was used as a power source to drive the cross-flow fan. It has an air supply system, a test cell, and a data acquisition system. The air supply system consisted of an electric motor which drove an Allis-Chalmers 12-stage axial compressor at 12,000 RPM through a gearbox. The compressor was capable of providing 3 atmospheres of air pressure which was fed into the turbine of the Space Shuttle Main Engine High-Pressure Fuel Turbopump. It was convenient to use this turbine in place of disassembling it for purposes of conducting the cross-flow fan test. Therefore, the only change needed was to provide a longer aluminum splined drive shaft, which transferred power to the CFTA. In this way, the existing bearing housing, associated bearing temperature and vibration monitoring systems, and the installed measurement system remained unmodified. A front view of the CFTA is shown in Fig. 5. The inlet bellmouth had a two-to-one elliptic section with a throat diameter of 158 mm (6.25 in). The transparent plexiglas window, which was used for flow visualization, is also shown in Fig. 5.

Fig. 5, Front view of CFT showing inlet bellmouth (top) and exhaust throttle (left)

INSTRUMENTATION

The instrumentation for data collection consisted of five United Sensor Devices model USD-C-161 3 mm (1/8-inch) combination thermocouple/pressure probes (combination probes), 12 static pressure taps, and the TTR total pressure, total temperature, and once-per-revolution measurement systems. The inlet elliptic bellmouth was instrumented with three static pressure taps at the throat of the inlet to measure mass flow rate.

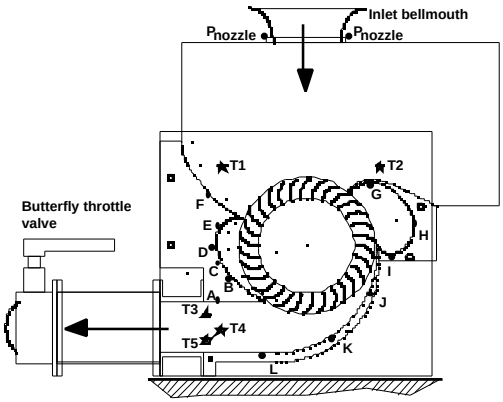

Fig. 6. Schematic of the CFTA showing location of the measurement probes.

Two combination probes (T1 and T2) were installed at roughly the 10 o'clock and 2 o'clock positions in the test assembly intake section, aligned with the anticipated flow direction, as shown in Figure 6. Three combination probes (T3 – T5) were installed in the exhaust duct section to detect pressure or temperature profiles in the exhaust duct. They were mounted such that the pitot opening of each probe was at the mid-point between the front and back plate. Twelve static pressure taps (A – L) were located at mid span at various locations around the cavities and exhaust section.

Flow patterns in the areas viewable through the Plexiglas viewing window were visualized using dye injection methods. Additional equipment included a video camera and digital still cameras for recording flow visualization results. Details of the data acquisition system and probe locations can be found in reference [8].

TEST PROCEDURE AND PROGRAM

Initial open throttle tests were conducted up to 7,000 rpm so as to compare the performance to that measured by VSD [7]. Flow visualization was performed at 5,000 rpm as this was thought to be the most efficient operating point as well as the speed at which the initial CFD solutions were targeted. Details of the test procedure are described by Seaton [8]. Peak efficiency was determined to be around 3,000 rpm so various test were performed with the throttle open but with different combinations of the cavities blanked off. Details of these tests can be found in reference [9].

The results presented in this paper are for two configurations, the baseline configuration with both cavities open and the other with both cavities blanked off. Throttling was performed from full open to stall for 2,000 – 6,000 rpm range (in 1,000 rpm increments).

The fan input power was obtained from

$$P_{CFF} = \dot{m}_{CFF} C_p \left(T_{out,\,CFF(avg)} - T_{in,CFF(avg)} \right) \quad (1)$$

where the mass flow rate, $\dot{m}_{CFF}$, was obtained from the inlet bellmouth and the inlet total temperature, $T_{in,CFF(avg)}$, was the average between the two inlet combination probes. The exit total temperature, $T_{out,\,CFF(avg)}$, was mass averaged from the three combination probes in the exhaust duct. This information allows one to determine the total compression efficiency defined as

$$\eta_{tt} = \frac{V \Delta p_{tt}}{P_{CFF}} \quad (2)$$

where V is the volume flow rate and Δp_{TT} is the total pressure rise through the fan (inlet averaged and exit mass averaged). This efficiency is identical to the total-to-total isentropic efficiency for incompressible flow. Both types of efficiency were calculated with little difference between the two for the range of speeds tested.

RESULTS AND DISCUSSION

Flow visualization was performed at a rotational speed of 5,000 RPM to obtain an understanding of the major flow features in the cross-flow fan. In Figure 7 the visualization due to three dyes injected in the left, center, and right ports of the Plexiglas inner blank is shown. To some extent, the vortex in the high pressure cavity (left side) and the low pressure cavity (right side) is also visible. Overlaying the flow pattern published by Vought Systems , shown in Figure 8, indicates that the flow through the test fan and the locations of the high and low pressure vortices are similar to the flow features in the Vought fan. It is also of interest to understand the changes in flow patterns with changes in mass flow.

As the flow through the fan was throttled, at 3,000 rpm, the following changes were observed, as shown in Figure 9 a and b. At peak efficiency the streamlines through the center of the rotor were well behaved, i.e. curved toward the exit. There is a small vortex located in the lower left hand portion of the rotor outside of the high pressure cavity. At stall the extent of

the vortex had grown to encompass most of the center of the rotor. The streamline patterns were also very irregular indicating that the flow was more unsteady at stall.

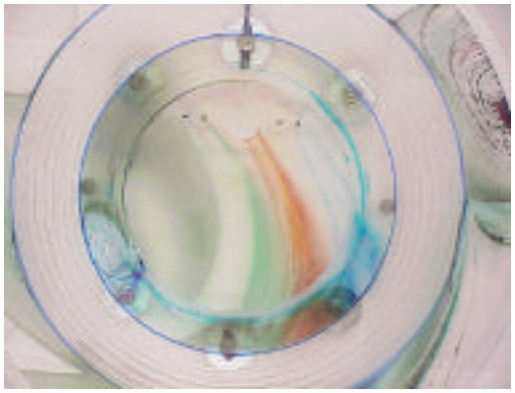

Fig. 7. Flow visualization patterns at 5,000 rpm

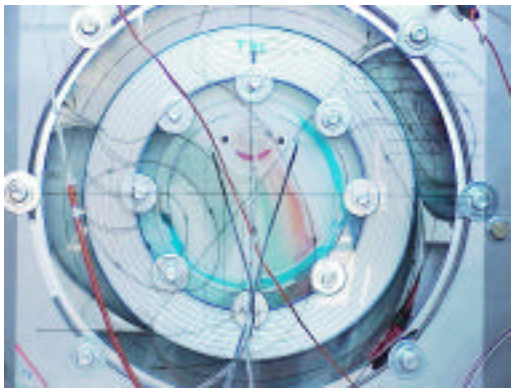

Fig. 8. Overlay of streamline patterns after reference [6].

The initial tests at 7,000 rpm compared favorably with those presented by VSD. The compression efficiency measured by Seaton [8] was slightly down (68% vs 71% by VSD) and the total pressure ratio was up (1.33 vs 1.29 by VSD), while the mass flowrate was identical at 1.12 kg/sec (2.48 lbm/sec). These measurements were performed without the inlet nozzle and exit throttle installed. The efficiency improved by four points and the pressure ratio dropped by about 1% at 6,000 rpm once the inlet nozzle and exhaust throttle were installed.

Starting from full open on the throttle, for each speed, the total pressure dropped as the mass flow rate was decreased as shown in the first plot of Fig. 10a. This characteristic is similar to centrifugal compressors, which have forward swept vanes [3]. For the baseline case the characteristic started out relatively flat and then increased in slope as the fan was taken into

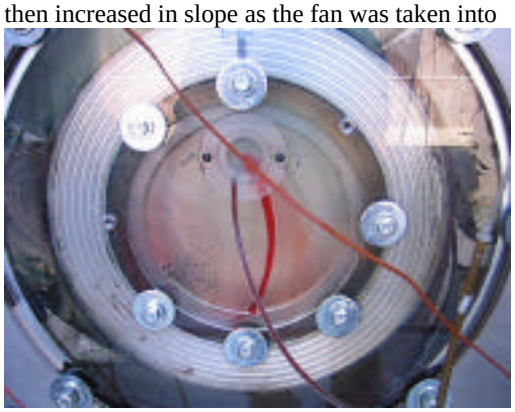

Fig. 9a. Flow visualization at peak efficiency at 3,000 rpm.

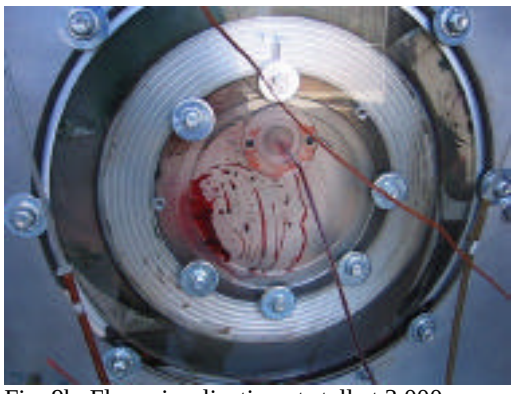

Fig. 9b. Flow visualization at stall at 3,000 rpm.

stall (the last point on the curve). In contrast, the configuration with the cavities blanked off exhibited nearly linear behavior with throttling over the whole speed range tested as shown in the first plot of Fig. 10b. This configuration produced a slightly lower peak pressure ratio (1.23 vs 1.27) and mass flow rate (1.02 kg/sec vs 1.08 kg/sec) at 6,000 rpm than the baseline configuration. Similarly, the temperature ratio for the baseline configuration (Fig. 10a) showed a non-linear behavior when compared to the blanked off configuration (Fig. 10b), particularly for the two highest speed lines of 5,000 and 6,000 rpm. The sharp increase in temperature ratio across the baseline configuration at stall resulted in a sharp drop in efficiency at stall from a peak value around 70% to below 30%. The configuration with the cavities blanked off had a slightly higher peak efficiency in the mid 70% range which did not decrease as noticeably near stall.

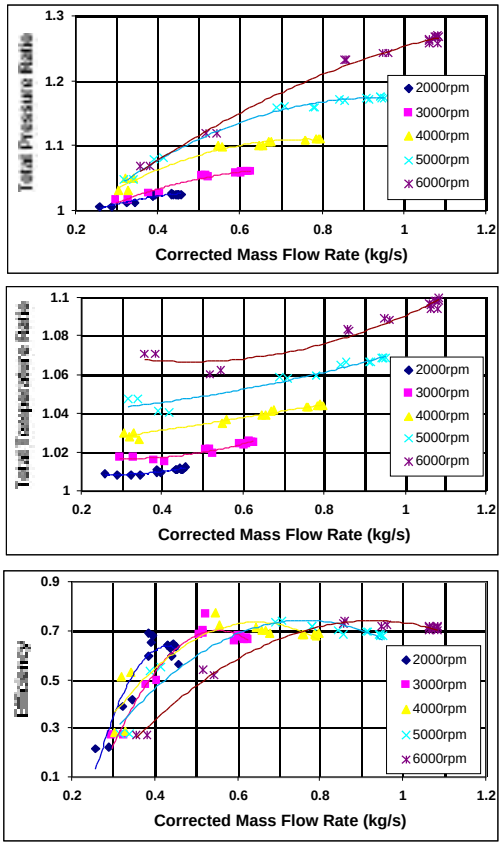

Fig. 10a. Total pressure and total temperature ratio and efficiency versus mass flow rate for the baseline geometry.

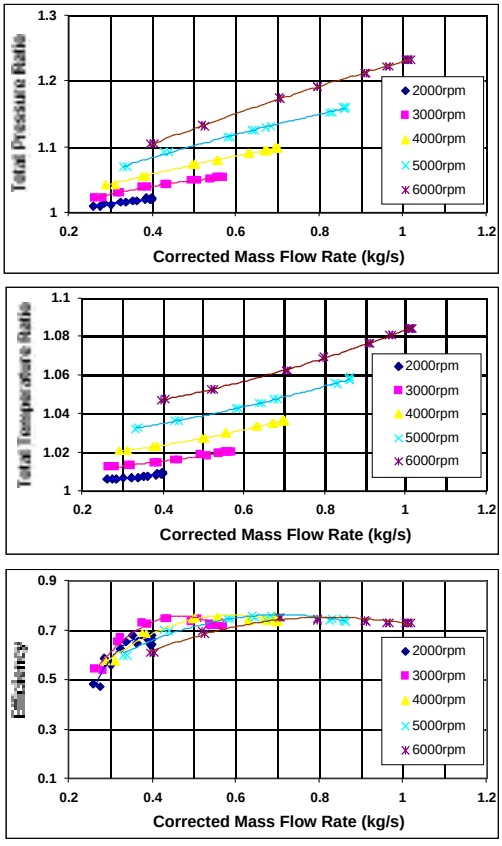

Fig. 10b, Total pressure and total temperature ratio and efficiency versus mass flow rate for both cavities blanked off.

The thrust versus mass flow rate plot for the baseline configuration (Fig. 11a) almost collapsed onto a single curve, which surprisingly was the case for the configuration with the blanked cavities as shown in the first plot of Figure 11b. This indicated that the same thrust could be obtained with the fan operating at 5,000 rpm at full open throttle versus the rotor turning at 6,000 rpm at partial mass flow rate. However; the 5,000 rpm operation was at a reduced power consumption of 15 kW versus 18 kW at 6,000 rpm. The maximum thrust-to-power ratio (N/kW) for the baseline configuration was 20.4 at 2,000 rpm and open throttle, which decreased to 6.9 at 6,000 rpm. These values were slightly up, 23.6 and 7.7 respectively, for the blanked-off configuration. The conclusion here being that if vertical lift thrust is required for a minimum power consumption, then slow rotor operation is required.

The total pressure and temperature profiles at the exit of the baseline configuration are plotted in figures 12 and 13 respectively. The rotational speed was 3,000 rpm and the data were taken at open throttle, peak efficiency (to coincide with the flow viz) and at stall. The total pressure distribution remained relatively uniform over the operating range, showing slight skewness at open throttle. However; the total temperature profile showed significant skewness at stall, having started out as a relatively symmetric profile.

The surface static pressures are tabulated in the Appendix (Table A1) for the three test cases, open throttle, peak efficiency and stall at 3,000 rpm. The labeling for these pressures is given in Fig. 6.

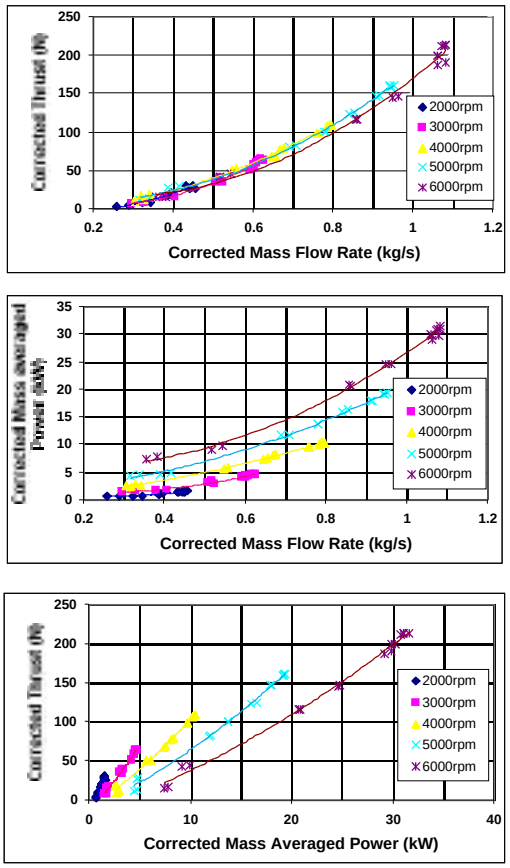

Fig. 11a, Corrected thrust, and power vs mass flow rate and thrust vs power for the baseline configuration.

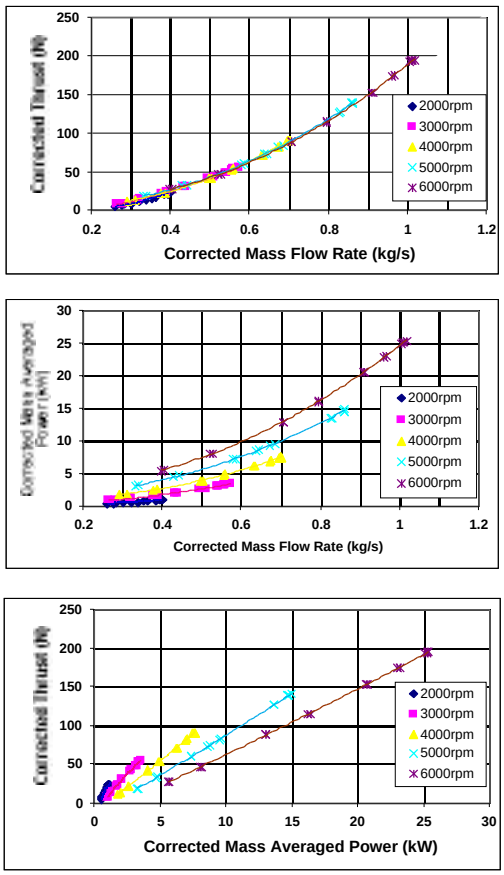

Fig. 11b, Corrected thrust, and power vs mass flow rate and thrust vs power for both cavities blanked off.

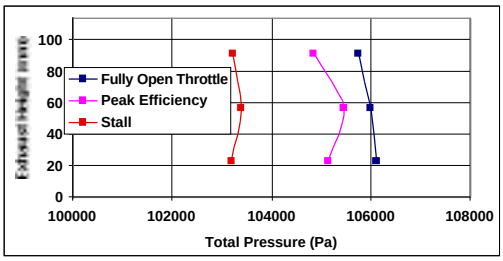

Fig. 12, Baseline exit plane total pressure distributions at 3,000 rpm.

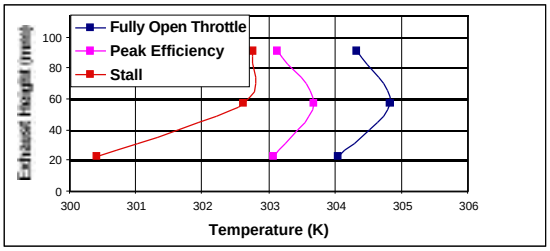

Fig. 13, Baseline exit plane total temperature distributions at 3,000 rpm.

COMPUTATIONAL ANALYSIS OF CROSS-FLOW FAN

A commercial PC-based computational fluid dynamics software package Flo++ developed by Softflo, was used to conduct a 2-D numerical simulation on the CFF. The 0.305 m (12-inch) diameter and 30-blade CFF, similar to that from the experimental setup, was modeled and run at a speed of 3000rpm. Incompressible and turbulent flow using a time marching upwind differencing modified PISO algorithm was used to solve the CFF unsteady cases. For turbulent flow calculations the high Reynolds number k-ε model is incorporated. Sliding meshes are used to model moving or rotating machinery.

Figures 14 and 15 show the 2-D computational grid and boundary groups for the CFF respectively. The boundaries used included inlet (purple), outlet(yellow), walls (white), and attached (orange and blue). The boundaries of type attached were used for sliding meshes where two groups of grids slid against each other. From Figure 16, the inlet and outlet boundary conditions were set to (0.97 bar and 300K) and (1bar and 300K) respectively. The reason for creating a pressure gradient was to bring the flow into the fan on the onset of the solution and thus assisting the solver computation in the initial stage. Details of the grid generation are given by Seaton [8]. A total of 58,600 vertices and 27,130 cells were used.

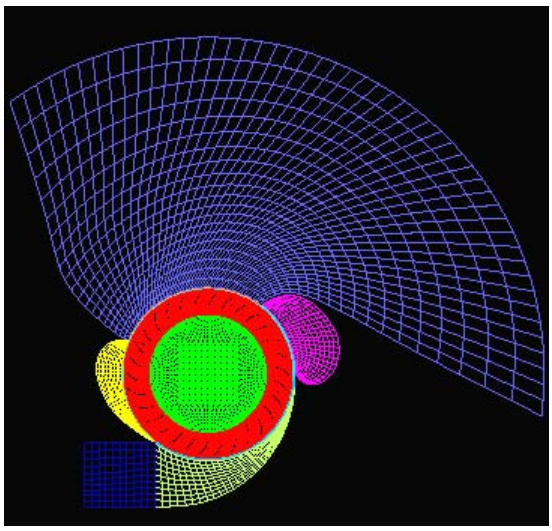

Fig. 14, Complete computational grid

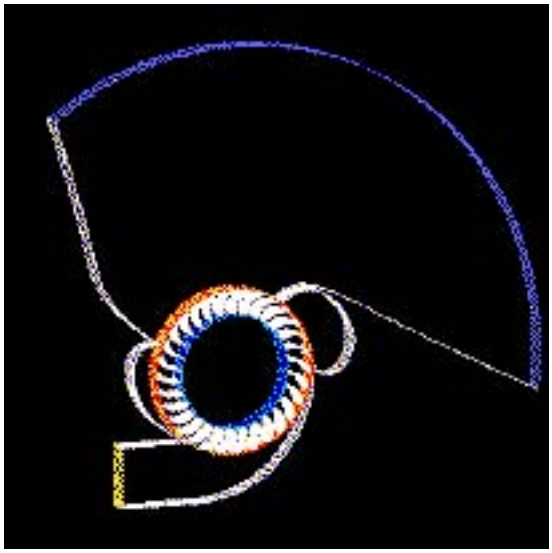

Fig. 15, Outline of grid showing boundary groups

Figure 16 shows the contour plot of the total pressure for the model. The figure illustrates the solution after eight revolutions which was assumed to be stable based on the nearly converged behavior of the total-to-total pressure ratio versus the number of revolutions plots as shown in Figure 17. Eight revolutions corresponded to 138,900 iterations at an average time step of approximately 1.1×10^{-6} sec. The re-circulation of flow vortices within both cavities were observed to be similar to those obtained from experiment. The lowest pressure occurred at locations just outside the left cavity, which justifies its name as the Low Pressure Cavity. The vortical flow features in the two cavities are displayed in more detail in Figures 18 and 19, which are very similar to those observed during the flow visualization measurements as shown in Figs. 7 and 8.

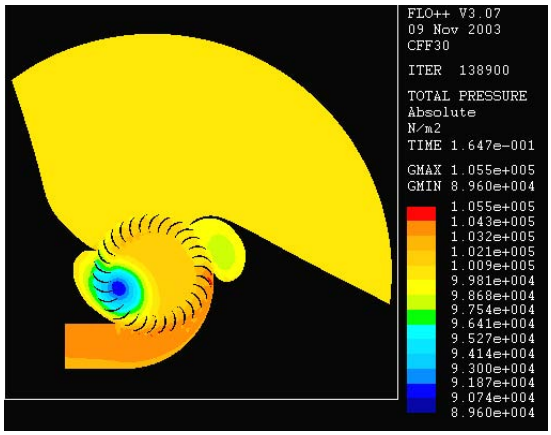

Fig. 16, Total pressure distribution for the baseline configuration at 3,000 rpm.

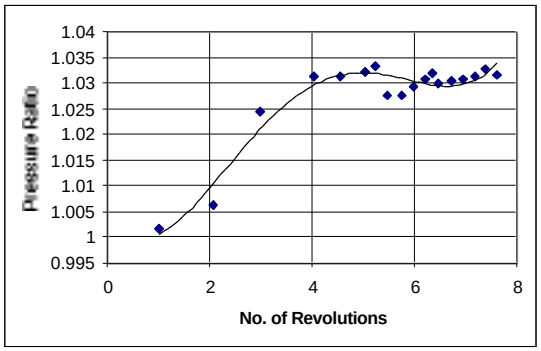

Fig. 17, Total pressure variation with number of revolutions during the computational simulation.

The predicted total pressure ratio for this case was 1.033 versus the measured value of 1.061. The predicted mass flow rate was 0.45 kg/sec versus the measured value of 0.615 kg/sec. Grid resolution and turbulence model and the difficulty of computing the flow details between rotor and housing are likely reasons for the lack of agreement with experiment.

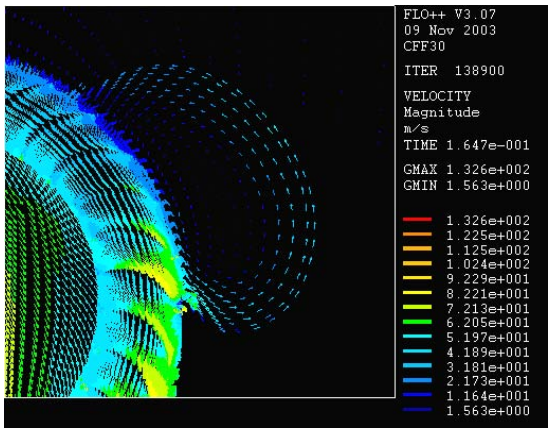

Fig. 18, Velocity vector plot in the Low-Pressure Cavity and Recirculation Area

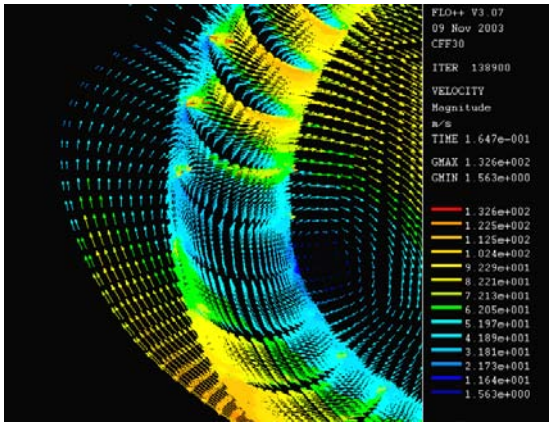

Fig. 19, Vector Plot of Velocity in the High-Pressure Cavity

SUMMARY AND OUTLOOK

The chosen baseline configuration described above was the same as that tested by Vought Systems Division. While the VSD rotational speeds ranged from 7,000 to 13,000 rpm the present tests covered the speed range up to 7,000 rpm. The results showed that at 7,000 rpm the present measurements closely reproduce the VSD results. The measured efficiencies were slightly in excess of 70%. This result is encouraging because at these relatively low rotational speeds the use of CFFs for aircraft propulsion purposes is likely to be advantageous from a performance and noise point of view.

Based on Gossett's [6] suggestion that a personal air vehicle will weigh about 5.8kN (1,300lbf) and his statement that a 1.3 thrust margin is needed for vertical take off, then 7.5kN

of thrust is needed from the CFF for vertical take off. At 3,000 rpm a thrust of 55.6 Newtons was measured (for the 38mm span CFF) and a Thrust-to-Power ratio of 16 N/kW, so 469 kW (628 hp) is needed to drive the CFF to produce 7.5 kN thrust. Then a total length of fan 5 m (~17 ft) is needed. While the length may be long the power required is very reasonable, as Moller [5] needs 481 kW (645 hp) to drive the Volantor.

The table below lists the various CFF speeds and estimated total length and power required for a vertical lift-off propulsion system.

Table 1

CFF revolutions per minute	CFF length [m] (ft)	Engine Power [kW] (hp)
2,000	12 (38)	318 (426)
3,000	5 (17)	469 (628)
4,000	3 (10)	625 (838
5,000	2 (6.6)	789 (1058)
6,000	1.5 (4.8)	974 (1306)

A complete performance map has been measured and generated for the two configurations described. These data as well as the associated flow visualization and probe measurements will make a valued data set for ongoing numerical predictions.

The preliminary Navier-Stokes computations described in this paper show that it is possible to reproduce the measured flow patterns. However, much more work is required to accurately predict the performance.

Future tests will include variations of the exhaust duct and other cavity configurations. Also tests of lower diameter CFFs will be performed in view of their easier installation in aircraft wing sections.

ACKNOWLEDGMENTS

The authors gratefully acknowledge the support of this investigation by the NASA Glenn Research Center, monitored by Mr. Gary Skoch.

REFERENCES

1. Ackeret, J., "Present and Future Problems of Aircraft Propulsion," *Schweiz. Bauztg.*, No. 1., 1938.
2. Eck, B., "Fans; Design and Operation of Centrifugal, Axial-Flow and Cross-Flow Fans," Pergamon Press, 1973.
3. Peebles, P., "FanWing: the New Microlight Technology?" http://www.fanwing.com
4. Bushnell, D.M., "Frontiers of the 'Responsibly Imaginable' in (Civilian) Aeronautics," The 1998 AIAA Dryden Lecture, Jan. 1998.
5. Moller P.S., 'Airborne Personalized Travel Using Powered Lift Aircraft," SAE/AIAA Paper No. 985533, World Aviation Conference, September 28-30, 1998, Anaheim, CA, also: "Volantor Technology," Moller International, Feb. 1999.
6. Gossett, D.H., "Investigation of Cross Flow Fan Propulsion for Lightweight VTOL Aircraft," Masters Thesis, Department of Aeronautics and Astronautics, Naval Postgraduate School, Monterey, CA 93943, Dec. 2000.
7. Vought Systems Division, "One and One-Half Inch Span Fan Test," Vol. I, "Twelve Inch Span Fan Test," Vol. II, "Multi-Bypass Ratio Propulsion System Technology Development," Vol. IV, prepared under contract N00019-74-C-0434 for Naval Air Systems Command, July 1975.
8. Seaton, M. S., "Performance Measurements, Flow Visualization, and Numerical Simulation of a Cross-Flow Fan," Masters Thesis, Department of Aeronautics and Astronautics, Naval Postgraduate School, Monterey, CA 93943, March 2003.
9. Cheng, W-T., "Experimental and Numerical Simulation of a Cross-Flow Fan," Masters Thesis, Department of Mechanical and Astronautical Engineering, Naval Postgraduate School, Monterey, CA 93943, Dec. 2003.

APPENDIX

Table A1. Static pressures on the cavities at 3,000 rpm for the baseline configuration

Port	Open Throttle	Peak Efficiency	Stall
PA [Pa]	100295	102033	102629
PB [Pa]	97928	99470	99917
PC [Pa]	97792	99451	100334
PD [Pa]	97767	99492	100447
PE [Pa]	97978	99758	100563
PF [Pa]	100268	100588	100856
PG [Pa]	100787	101167	100918
PH [Pa]	101420	101610	101225
PI [Pa]	102056	102319	101700
PJ [Pa]	100930	101430	101049
PK [Pa]	100920	100923	100876
PL [Pa]	100856	100871	100876